

Article

Not peer-reviewed version

# Wnt/Beta-Catenin Signaling Regulates Hepatitis B Virus cccDNA Levels

[Atsuya Ishida](#) , [Sadahiro Iwabuchi](#) , Yiang-Yi Li , [Kazuhisa Murai](#) , [Takayoshi Shirasaki](#) , Kazuyuki Kuroki , [Tetsuro Shimakami](#) , [Koki Nio](#) , [Kazunori Kawaguchi](#) , Tadashi Imafuku , Satoru Ito , [Taro Yamashita](#) , Shuichi Kaneko , Hiroshi Yanagawa , Kouji Matsushima , [Masao Honda](#) <sup>\*</sup> , [Shinichi Hashimoto](#)

Posted Date: 4 June 2025

doi: 10.20944/preprints202506.0173.v1

Keywords: Hepatitis B virus; cccDNA; DOCK11; TNKS; beta-catenin



Preprints.org is a free multidisciplinary platform providing preprint service that is dedicated to making early versions of research outputs permanently available and citable. Preprints posted at Preprints.org appear in Web of Science, Crossref, Google Scholar, Scilit, Europe PMC.

Copyright: This open access article is published under a Creative Commons CC BY 4.0 license, which permit the free download, distribution, and reuse, provided that the author and preprint are cited in any reuse.

## Article

# Wnt/Beta-Catenin Signaling Regulates Hepatitis B Virus cccDNA Levels

Atsuya Ishida <sup>1,†</sup>, Sadahiro Iwabuchi <sup>2,3,†</sup>, Yiang-Yi Li <sup>4</sup>, Kazuhisa Murai <sup>1</sup>, Takayoshi Shirasaki <sup>1</sup>, Kazuyuki Kuroki <sup>4</sup>, Tetsuro Shimakami <sup>4</sup>, Koki Nio <sup>4</sup>, Kazunori Kawaguchi <sup>4</sup>, Tadashi Imafuku <sup>3</sup>, Satoru Ito <sup>5</sup>, Taro Yamashita <sup>4</sup>, Shuichi Kaneko <sup>4</sup>, Hiroshi Yanagawa <sup>5</sup>, Kouji Matsushima <sup>6</sup>, Masao Honda <sup>1,4,\*</sup> and Shinichi Hashimoto <sup>3</sup>

<sup>1</sup> Department of Clinical Laboratory Medicine, Kanazawa University Graduate School of Medical Sciences, Kanazawa, Japan

<sup>2</sup> Department of Bioinformatics and Genomics, Graduate School of Advanced Preventive Medical Sciences, Kanazawa, Japan

<sup>3</sup> Department of Molecular Pathophysiology, Institute of Advanced Medicine, Wakayama Medical University, Wakayama, Wakayama, Japan

<sup>4</sup> Department of Gastroenterology, Kanazawa University Graduate School of Medicine, Kanazawa, Ishikawa, Japan

<sup>5</sup> Purotech Bio Inc., Yokohama, Kanagawa, Japan

<sup>6</sup> Division of Molecular Regulation of Inflammatory and Immune Disease, Research Institute for Biomedical Sciences, Tokyo University of Science, Noda, Chiba, Japan

\* Correspondence: mhonda@m-kanazawa.jp; Tel: +81-76-265-2601

† These authors contributed equally to this study.

**Abstract:** Hepatitis B virus (HBV) specifically infects hepatocytes and has a complex life cycle owing to the stabilization and pooling of covalently closed circular DNA (cccDNA) in the nucleus of infected hepatocytes. We previously reported that the suppression of dedicator of cytokinesis 11 (DOCK11) decreases cccDNA and HBV-DNA levels and identified it as a new HBV therapeutic target. The DOCK11-associated gene, Wnt/ $\beta$ -catenin signaling regulator tankyrase (TNKS), was identified using in vitro methods; however, its function in the HBV life cycle remains unknown. Here, we used various inhibitors, antagonists, and short-hairpin RNA treatments related to TNKS signaling in HBV-infected hepatocytes. The role of TNKS-related Wnt/ $\beta$ -catenin signaling in the HBV life cycle was evaluated using immunoprecipitation assays with DOCK11 and bulk RNA sequencing methods. TNKS and Wnt/ $\beta$ -catenin signaling inhibitors significantly repressed cccDNA and HBV-DNA levels. Conversely, certain Wnt/ $\beta$ -catenin signaling agonists enhanced the HBV life cycle. DOCK11 directly binds to  $\beta$ -catenin to regulate HBV using its nuclear transport system. SKL2001, normally used as a Wnt/ $\beta$ -catenin signaling agonist, strongly reduced cccDNA expression in HBV-infected hepatocytes and in combination with entecavir predominantly eradicated HBV without cytotoxicity. Therefore, DOCK11 and other Wnt/ $\beta$ -catenin signaling molecules may be therapeutic targets to prevent persistent HBV infection.

**Keywords:** Hepatitis B virus; cccDNA; DOCK11; TNKS; beta-catenin

## 1. Introduction

Chronic hepatitis B virus (HBV) infection is a leading cause of liver cirrhosis and hepatocellular carcinoma (HCC) worldwide. The key to persistent HBV virology is an intracellular HBV replication intermediate, called covalently closed circular (ccc) DNA, which exists as a stabilized plasmid-like molecule in the nucleus of HBV-infected cells and gives rise to progeny viruses [1]. Thus, to completely cure chronic HBV, cccDNA must be removed. A mean of around 0.1–1.0 or 10 copies per cell is detected in HBV-infected human liver chimeric mice or duck liver, respectively [2]. However,

the molecular mechanisms underlying cccDNA formation and degradation, remain unclear. We previously reported that knockdown of dedicator of cytokinesis 11 (DOCK11), which encodes small GTPase regulators, strongly decreased the levels of both cccDNA and HBV-DNA levels in HBV-infected primary human hepatocyte (PXB) cells [3–6]. DOCK11 is a specific guanine nucleotide exchange factor for Rho GTPase of the cell division cycle 42 (CDC42) and cccDNA synthesis is regulated by CDC42 and activated CDC42-associated kinase 1 [5]. DOCK11 and CDC42 also regulate the retrograde trafficking of HBV from the Golgi to the endoplasmic reticulum (ER) [4]. Additionally, combination treatment with entecavir and DOCK11 depletion significantly restricts cccDNA levels compared to treatment with either drug alone in patients with chronic HBV infection [4,6]. However, the effects of DOCK11 and DOCK11-binding proteins other than CDC42 on the cccDNA life cycle remain unknown. Moreover, in the development of DOCK11-targeted inhibitors for cccDNA eradication, a detailed understanding of DOCK11-related signaling in cells will lead to the consideration of potential side effects. Here, we focused on tankyrase (TNKS) which was screened and identified as a DOCK11-associated protein using an in vitro viral method [7].

TNKS consists of two members (TNKS1 and TNKS2) and is a poly (ADP-ribose) polymerase (PARP) that regulates PAR chains via catalytic action [8]. TNKS binds to PARylated axins, which are subsequently ubiquitinated and degraded [9]. TNKS suppresses cancer progression through inhibiting the Wnt/ $\beta$ -catenin signaling pathway [10]. A key feature of Wnt/ $\beta$ -catenin signaling is the regulated proteolysis of the downstream effector  $\beta$ -catenin by the  $\beta$ -catenin destruction complex [11]. The constituents of the  $\beta$ -catenin destruction complex are adenomatous polyposis coli (APC), axins, and glycogen synthase kinase  $3\alpha/\beta$  (GSK- $3\alpha/\beta$ ). In the absence of Wnt pathway activation, axins binds to GSK- $3\beta$  and cytosolic  $\beta$ -catenin at Ser45 and Ser33/37/Thr41 in which are constitutively phosphorylated by GSK- $3\beta$  and targeted for degradation [12]. Axin inhibition by TNKS suppresses  $\beta$ -catenin phosphorylation. Conversely, the interaction of various Wnts with their receptors triggers axin detachment from the  $\beta$ -catenin destruction complex, leading to the inhibition of  $\beta$ -catenin phosphorylation [11,12]. This enhances the accumulation of nuclear  $\beta$ -catenin and transcription of Wnt pathway-responsive genes. Wnt/ $\beta$ -catenin signaling pathway modulates HBV biosynthesis [13,14]. Liver-specific  $\beta$ -catenin-null HBV transgenic mice lack significant reduction of viral DNA replication and  $\beta$ -catenin regulates liver receptor homolog 1 (LRH1)-mediated transcription from the HBV core promoter [14]. In addition,  $\beta$ -catenin enhances LRH1 and farnesoid X receptor  $\alpha$  (FXR $\alpha$ )-mediated activated transcription and replication of HBV in the human hepatoma Huh7 cell line [13]. However, the details regarding Wnt/ $\beta$ -catenin signaling and HBV replications in other HBV-infected hepatocytes remain unknown.

In the present study, we investigated whether DOCK11-associated protein TNKS and Wnt/ $\beta$ -catenin signaling could regulate cccDNA and HBV-DNA levels in two cell lines; HBV-infected PXB and HepG2.2.15 cells [15,16]. We also examined how various Wnt/ $\beta$ -catenin signaling inhibitors and agonists affects the HBV lifecycle and whether they are effective in combination with entecavir.

## 2. Results

### 2.1. Inhibition of TNKS eliminated HBV cccDNA

To investigate the potential effects of TNKS inhibitors on cccDNA and HBV-DNA, we applied 0.1 mM of XAV939 to PXB cells (Figure 1A) and 10 mM XAV939 to HepG2.2.15 cells (Figure 1B). Compared to control cells treated with dimethyl sulfoxide (DMSO), cccDNA and HBV-DNA levels were significantly lower ( $p < 0.001$ ) in both cell lines. The DMSO concentration of culture medium in PXB and HepG2.2.15 cells was less than 0.05%. XAV939 was applied from d 1 to d 12 to HBV-infected PXB cells, and the medium was changed on d 6. Conversely, HepG2.2.15 cells were treated with TNKS inhibitors for 12 d and medium was changed on d 4 and 8. About 60% or 67% suppression of cccDNA or HBV-DNA was observed in XAV939-treated PXB cells (Figure 1A). In HepG2.2.15 cells, the cccDNA copy number of DMSO or XAV939-treatment groups was  $8.5 \times 10^8 \pm 6.3 \times 10^6$  and  $4.4 \times 10^8 \pm 2.8 \times 10^6$  (mean  $\pm$  S.E.), respectively (Figure 1B). DNA copy number decreased about 66% with

XAV939 treatment. To examine the dose-dependent effects of XAV939 on cccDNA and HBV-DNA suppression in each cell line, we treated PXB cells with XAV939 (10–25 mM) (Figure 1C) or HepG2.2.15 cells with 10–100 mM (Figure 1D). XAV939 was lethal at concentrations above 25 mM in PXB cells or 100 mM in HepG2.2.15 cells, and the final DMSO concentration in each culture medium was 0.125 or 0.5%, respectively. Thus, the concentration of XAV939 that significantly reduced both cccDNA and HBV-DNA expression was used in subsequent experiments. The effect of XAV939 on TNK1/2 and HBsAg protein levels in PXB cells was determined using western blotting (Figure 1E). The expression level of TNK1/2 was unaffected; however, HBsAg levels were significantly reduced. RNA-seq results showed that *TNKS* or *TNKS2* mRNA levels in HBV-infected PXB cells were slightly increased (1.08 or 1.25-fold changes, respectively) (Supplementary Data S1). To further investigate the effect of TNKS inhibition on cccDNA and HBV-DNA, we used four other representative TNKS inhibitors [17–21]. The appropriate concentration of each TNKS inhibitor was determined based on cell viability using the MTT assay (Figure 1F). Compared to those in the DMSO loading group, cccDNA and HBV-DNA levels were significantly decreased in the 10 nM AZ6102 [20], 10 mM JW55 [17,21], 80 nM MN64 [18], and 50 nM G007-LK [19] treatment groups (Figure. 1G), strongly suggesting that TNKS is involved in regulating HBV production.

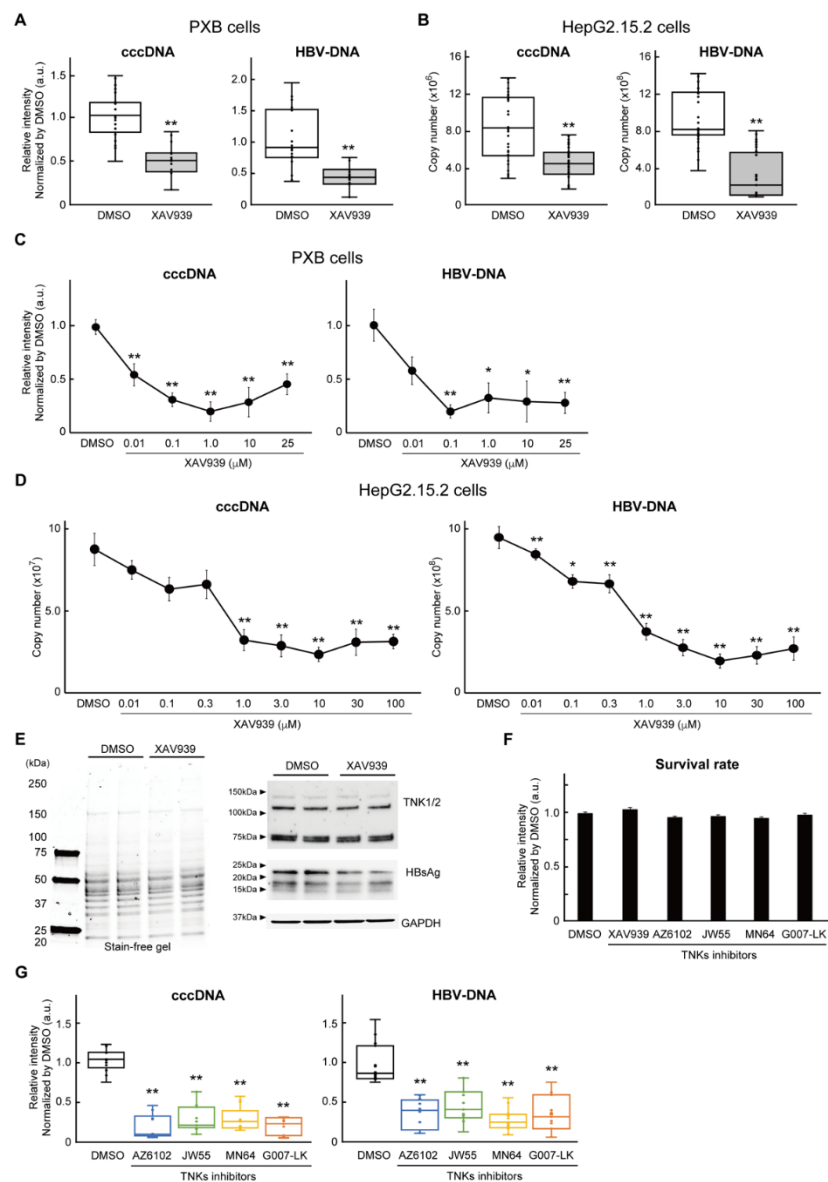


**Figure 1.** TNKS inhibitors decreased cccDNA and HBV-DNA levels. (A) Expression of cccDNA and HBV-DNA was measured in PXB cells using qPCR. The relative intensity (arbitrary unit; a.u.) was calculated by the normalization of each copy number in DMSO treatment groups. Bars indicate the mean  $\pm$  standard error (S.E.).



**\*\***,  $p < 0.01$  vs DMSO group. Number of cell culture batch (N) = 5, number of culture wells (n) = 16–24. **(B)** Graph showing the mean  $\pm$  S.E. of cccDNA and HBV-DNA copy numbers in DMSO or 10  $\mu$ M XAV939 treatment groups. **\*\***,  $p < 0.01$  vs DMSO group. N=8, n=41–47. **(C)** Dose-dependent effect of XAV939 on cccDNA and HBV-DNA levels in PXB cells. Y axis indicated relative intensity normalized by the copy numbers in DMSO treatment groups (a.u.). Bars indicate the mean  $\pm$  S.E. \* or **\*\***,  $p < 0.05$  or 0.01 vs DMSO group. N=3–8, n=5–24. **(D)** Graph showing the dose-dependent changes in cccDNA and HBV-DNA copy numbers in DMSO and XAV939 treatment groups. Bars indicate the mean  $\pm$  S.E. \* or **\*\***,  $p < 0.05$  or 0.01 vs DMSO group. N=5–8, n=6–47. **(E)** Protein levels of TNK1/2, HBsAg and GAPDH in PXB cells were determined using western blotting. The whole blotting image obtained using stain-free gel (left) and the expression of target proteins (right). Representative blotting images are shown, and each assay performed at least three times using different cell lysates. N=2, n = 6 in DMSO or XAV939 treatment groups. **(F)** Graph showing the relative intensity for survival rate (a.u.) in each inhibitor treatment groups normalized to the intensity in DMSO group. Survival rate (%) in each culture condition was obtained using the MTT assay, then normalized to the survival rate in the DMSO group. Bars indicate the mean  $\pm$  S.E. No significant difference was observed. N=3, n=8–10. **(G)** Expression of cccDNA and HBV-DNA was measured using qPCR in PXB cells with different TNKS inhibitors. Bars indicate the mean  $\pm$  S.E. **\*\***,  $p < 0.01$  vs DMSO group. N=4, n=10–14.

## 2.2. Identification of differentially expressed genes (DEGs) associated with TNKS inhibition

A total of 213 DEGs detected when comparing the two XAV939 treatment groups with the two DMSO groups (Supplementary Data S2). A total of 97 upregulated and 116 downregulated genes were identified according to the criteria ( $-\log_2$  fold change  $> 1.0$ ,  $p$ -value  $< 0.05$ ), and volcano curves were constructed to visualize the DEGs (Figure 2A). The heatmap shows the top 100 DEGs after hierarchical clustering across samples (Figure 2B), identifying the strongly upregulated and downregulated genes. This heatmap indicates that the changes in gene expression profiles in HBV-infected PXB cells treated with XAV939 were clearly different. Gene set enrichment analysis (GSEA) was performed to examine DEG profiles in detail. The advantage of GSEA is that it does not use a cutoff condition for detecting DEGs and the gene sets are significantly detected using whole-gene data, even though the changes in individual genes may be relatively subtle. Figure 2C shows an excerpted heat map of the top 50 features for each culture condition for the 230,213 genes. The genes most highly upregulated by XAV939 treatment were cytochrome P450 1A2 (*CYP1A2*) and 1A1 (*CYP1A1*), which are regulated by the Wnt/ $\beta$ -catenin pathway [22], possibly indicating that the signaling might be related to the removal of cccDNA and HBV-DNA. Conversely, XAV939 downregulated genes, such as *NFSP1*, *GJA1*, *KANK3*, and *WNN3*, which were possible candidate genes for regulating intracellular cccDNA maintenance. However, most of the genes affected by XAV939 treatment were lncRNAs or snoRNAs. Differences in individual gene expression were negligible, and the efficiency of HBV infection in PXB cells must be considered. GSEA revealed that 41/50 gene sets were upregulated in the DMSO group, and eight gene sets were significantly enriched (nominal  $p$ -value  $< 0.05$ ). The enrichment score (ES) line graph indicated the ES value of the gene set (Figure 2D) and the top three significantly enriched gene sets (mTORC1 complex, G2M checkpoint, and inflammatory response) were shown. In contrast, 9/50 gene sets were upregulated in the XAV939 treatment groups; however, only one gene set, xenobiotic metabolism, was significantly enriched (nominal  $p$ -value  $< 0.05$ ). Next, we performed Gene Ontology (GO) functional annotation of the DEGs using Metascape [23]. First, we calculated the ratio of the averaged TPM values between the two different DMSO and XAV939 treatment groups, and over 1.5-fold higher genes under each condition were applied to Metascape. The 968 genes upregulated in the DMSO groups, that is, downregulated in the XAV939 treatment groups, were annotated, and the functions of extracellular matrix regulation, such as NABA matrisome-associated ( $-\log_{10}p = 10.3$ ), extracellular matrix organization ( $-\log_{10}p = 10.2$ ), and NABA core matrisome ( $-\log_{10}p = 9.9$ ) were observed to be significantly enhanced. Conversely, the 816 genes upregulated in the XAV939 treatment induced the acceleration of cilium movement ( $-\log_{10}p = 10.1$ ), regulation of hormone levels ( $-\log_{10}p = 7.1$ ), and organic hydroxy compound metabolic processes ( $-\log_{10}p = 6.6$ ) and no significant connection was observed between

them. These results suggest that XAV939 treatment of HBV-infected PXB cells might activate signals, such as cell proliferation, inflammatory response, and extracellular matrix synthesis, leading to a reduction in cccDNA and HBV-DNA.

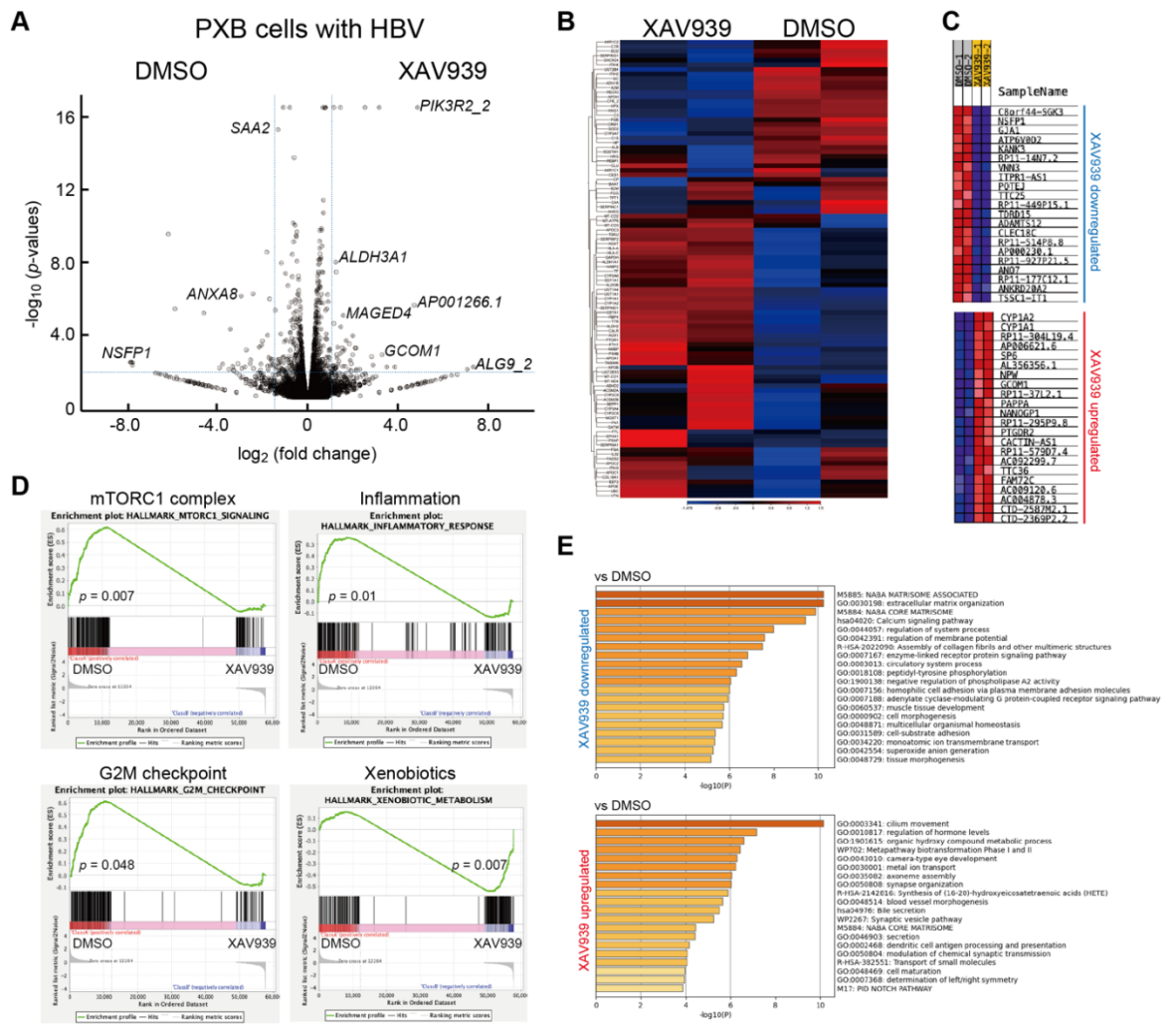


**Figure 2.** Differential expression analysis of RNA-seq datasets. **(A)** RNA-seq data were analyzed using the CLC Genomics Workbench, and the DGEs between the DMSO and XAV939 treatment groups were visualized using a volcano map. The definition of DEGs (blue dotted lines) was  $\log_2 \text{FC} > 1.0$  and  $-\log_{10}(p\text{-value}) > 2.0$ . We used two different RNA-seq datasets obtained from different PXB cells to detect DEGs. **(B)** Heatmap analyzed using CLC Genomics Workbench. The top 100 DEGs were identified. Left two rows: XAV939 treatment group; right two rows: DMSO treatment group. The red to blue scale bar indicates  $\log_2 \text{FC}$ . **(C)** Heatmap plots of the top 50 upregulated or downregulated DEGs obtained using gene set enrichment analysis (GSEA). Each heatmap shows only the top 20 extracted genes. The colors are row-normalized rank-ordered gene scores such that the maximum value for each gene is plotted in red and the minimum value is plotted in blue. **(D)** GSEA revealed pathways with one representative positive enrichment and three negative enrichments after XAV939 treatment relative to DMSO controls. The genes corresponding to the red part of the heat map were highly expressed in the DMSO treatment group, and the genes corresponding to the blue part were highly expressed in the XAV939 treatment group. The signal-to-noise ratio corresponding to each gene is shown in the gray area map. **(E)** Gene Ontology (GO) analysis using Metascape showed significantly downregulated (upper graph) and upregulated gene functions (lower graph) following XAV939 treatment. Bars indicate  $-\log_{10}(p\text{-value})$ . The TPM value of the gene in XAV939 treatment group was normalized to that of the DMSO (control) group. The value  $> 1.5$  set as threshold.

2.3. Wnt/ $\beta$ -catenin signaling regulates cccDNA and HBV-DNA levels

The XAV939 strongly regulates the Wnt pathway by inhibiting TNKS and subsequent destabilization of  $\beta$ -catenin levels [24]. Therefore, we next examined the effects of Wnt/ $\beta$ -catenin signaling inhibitors and activators on cccDNA and HBV-DNA levels in PXB cells. Representative inhibitors of Wnt/ $\beta$ -catenin signaling JW55 [25], JW67 [25], and salinomycin [26] significantly suppressed the cccDNA and HBV-DNA levels. Conversely, the activators of Wnt/ $\beta$ -catenin signaling, namely 10 mM Wnt agonist [27] and 50 mM HLY78 [28], strongly enhanced both levels (Figure 3A). The concentrations of each drug were not cytotoxic to the DMSO-treated groups (Figure 3B). To directly examine the relevance of  $\beta$ -catenin to the HBV virus, we applied lentiviral short hairpin RNA (shRNA) targeting  $\beta$ -catenin (*CTNNB1*) to HBV-infected PXB cells. The reduction of *CTNNB1* mRNA showed a slight decrease in cccDNA, though no change in HBV-DNA expression (Figure 3C), suggesting that  $\beta$ -catenin might regulate nuclear transport of rcDNA in the early stage of HBV infection. Stabilized  $\beta$ -catenin possesses the ability to translocate between nucleus and cytoplasm through the nuclear pore complexes (NPCs) [29]. The  $\beta$ -catenin directly binds to nuclear pore complex (NPC) proteins (nucleoporins), which are similar to importin- $\beta$  family members. NUP50 has been proposed to act as a cofactor for importin- $\alpha$  and importin- $\beta$  nuclear complex import cargo [30]. Importin- $\beta$  can infiltrate the HBV core dimer and empty capsids [31]. Both shRNA targeting NUP50 mRNA (shNUP50) and the inhibitor of importin- $\beta$  importazole (50 mM) [32] significantly decreased of cccDNA and HBV-DNA in HBV-infected PXB cells (Figure 3D). These results suggest that Wnt/ $\beta$ -catenin signaling was associated with the mechanism of HBV maintenance.

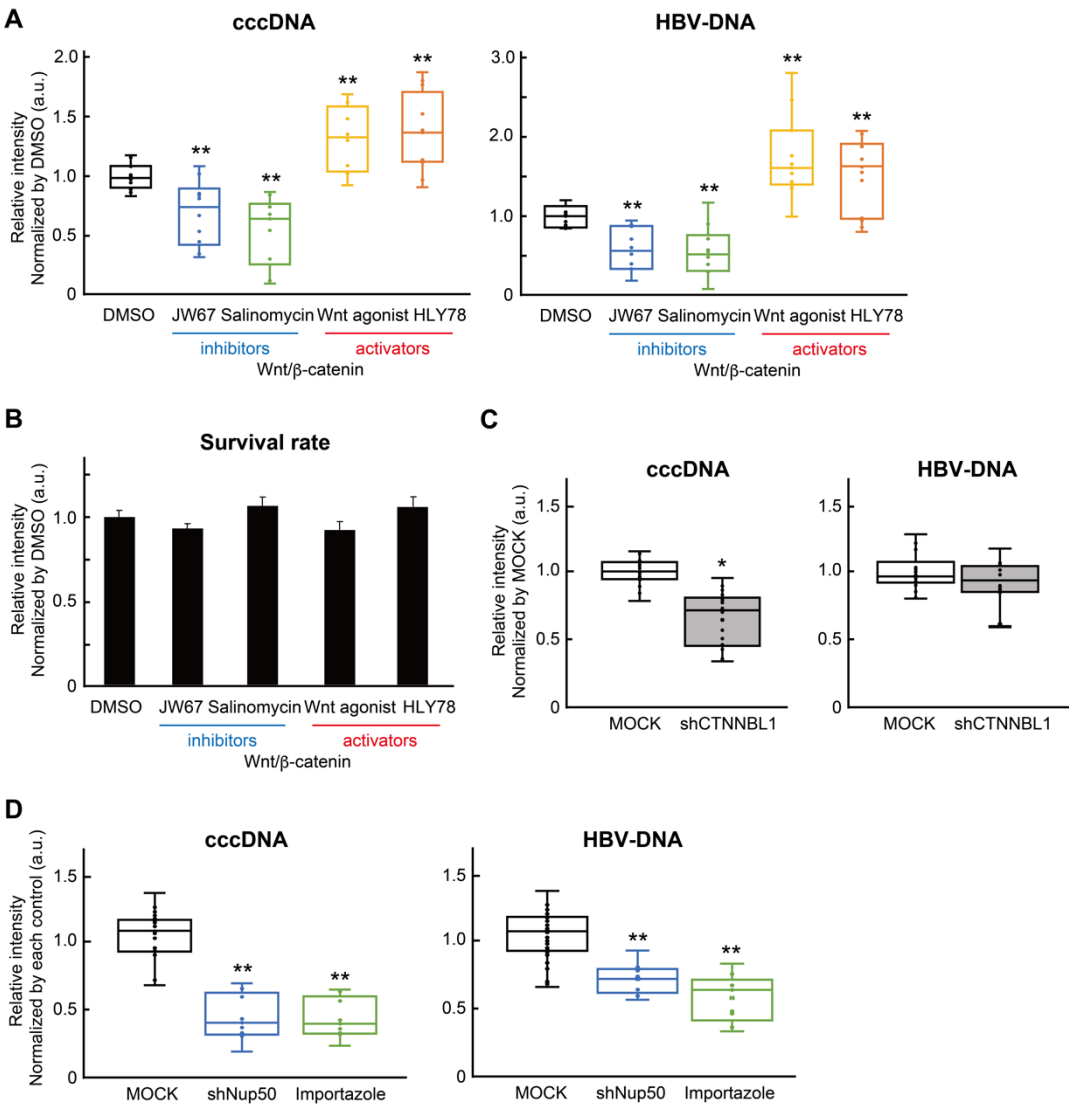


**Figure 3.** Involvement of Wnt/ $\beta$ -catenin signaling in HBV maintenance. (A) The effects of Wnt/ $\beta$ -catenin inhibitors and activators on cccDNA and HBV-DNA expression in PXB cells were evaluated using qPCR. The relative intensity (arbitrary unit; a.u.) was calculated by normalization to the each copy number in DMSO treatment groups. Bars indicate the mean  $\pm$  standard error (S.E.). \*\*,  $p < 0.01$  vs DMSO group. Number of cell culture batches (N) = 3, number of culture wells (n) = 8–11. (B) Graph showing the relative intensity for survival rate (a.u.) in each inhibitor treatment groups normalized to the intensity in the DMSO group. Survival rate (%) in each culture condition was obtained using an MTT assay, then normalized to the survival rate in the DMSO group. Bars indicate the mean  $\pm$  S.E. No significant difference was observed. N=3, n=8–11. (C) The copy number of cccDNA and HBV-DNA in shRNA for CTNNB1 (shCTNNB1) groups was normalized to those of MOCK groups. The graph showed the mean  $\pm$  S.E. of normalized copy number of cccDNA and HBV-DNA. \*,  $p < 0.05$  vs MOCK group. N=8, n=41–47. (D) The graph showed the mean  $\pm$  S.E. of copy numbers of cccDNA and HBV-DNA in MOCK, shRNA for Nup50 (shNup50) or importazole (50  $\mu$ M) treatment groups. \*\*,  $p < 0.01$  vs MOCK or DMSO group. N=4, n=4–6. Y axis indicates relative intensity normalized to the copy number in each control (MOCK for shNup50, DMSO for importazole) treatment groups (a.u.).

We previously showed that DOCK11 is essential for the maintenance of HBV in infected PXB cells and regulates unique HBV retrograde nuclear trafficking via Golgi-to-ER transport [4,6]. To investigate whether DOCK11 was associated with Wnt/ $\beta$ -catenin signaling, we performed IP assays with DOCK11 and  $\beta$ -catenin antibody in HBV-infected PXB and HepG2.2.15 cells. The mRNA expression of *DOCK11* and *CTNNB1* was relatively similar in control and HBV-infected PXB cells (Supplementary Data S1). As shown in Figure 4A, HBV infection did not alter DOCK11 and  $\beta$ -catenin protein levels. The IP assay using DOCK11 antibody in HBV-infected PXB cells and HepG2.2.15 cells clearly detected  $\beta$ -catenin protein (Figure 3B, 3C). In addition, the IP assay using  $\beta$ -catenin antibody also clearly detected DOCK11 protein in HepG2.2.15 cells (Figure 4D). In contrast, no correlation between DOCK11 and  $\beta$ -catenin expression levels was observed using HepG2-NTCP-C4-Halo-DOCK11 cell-derived lysate (Figure 4E). Immunofluorescence staining using DOCK11 and  $\beta$ -catenin antibody in HepG2.2.15 cells revealed co-localization of both in the cytoplasm and around the nuclear membrane (Figure 4F). Enrichment gene set analysis by using RNA-seq data indicated that no significant difference occurred for gene sets of Wnt/ $\beta$ -catenin signals in MOCK or shRNA for DOCK11-treated PXB cells (Supplementary Figure S2). DOCK11 regulates rcDNA transport from the cytoplasm to the nucleus, and DOCK11 and cccDNA co-localize in the nucleus [3]. Therefore, our results imply that DOCK11/ $\beta$ -catenin complex with rcDNA freely translocates between nucleus and cytoplasm through the NPCs.

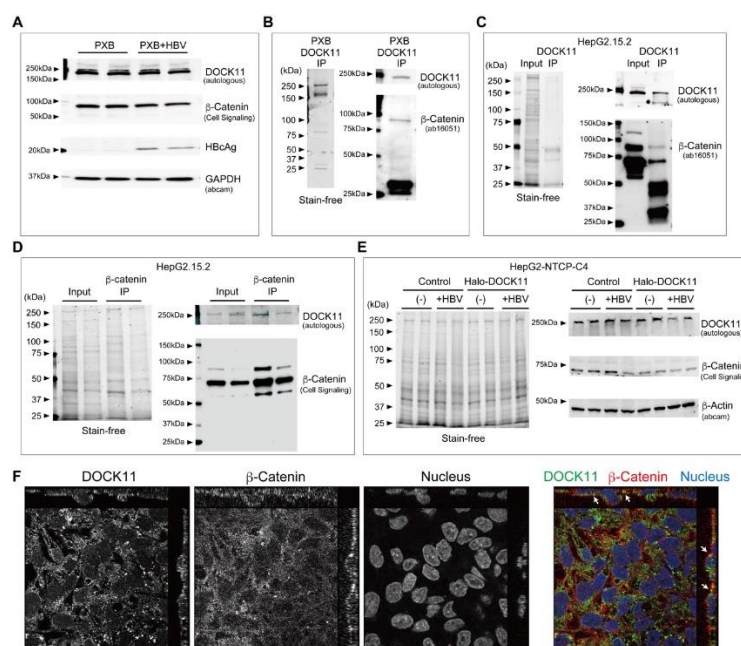




**Figure 4.** Interaction of  $\beta$ -catenin and DOCK11 proteins. (A) Protein levels of DOCK11,  $\beta$ -catenin, HBsAg, and GAPDH in PXB cells were determined using western blotting. The whole blotting image obtained using stain-free gel is shown in Supplementary Figure S1. Representative blotting images for PXB control or PXB with HBV infected groups are shown. The arrowheads indicate the size of bands (kDa). (B) Immunoprecipitation (IP) assays using DOCK11 in HBV-infected PXB cells. Whole gel image is shown (left). Western blotting using anti-DOCK11 or  $\beta$ -catenin antibody detected 250 kDa or 80 kDa, respectively (right). (C) IP assay using DOCK11 antibody in HepG2.2.15 cells. The whole stain-free gel image (left). Left lane: Input, right lane: IP for DOCK11. The lysate of IP by using DOCK11 antibody was then examined for co-expression by Western blotting with  $\beta$ -Catenin antibodies (right). (D) IP using  $\beta$ -Catenin antibody in HepG2.2.15 cells. Whole stain-free gel image is shown (left). Left lane: two inputs, right lane: two IP assays of  $\beta$ -catenin. DOCK11 was detected in the lysate of IP for  $\beta$ -catenin (right). (E) Immunoblotting of DOCK11,  $\beta$ -catenin, and  $\beta$ -actin in the cell lysate obtained from HepG2-NTCP-C4, HepG2-NTCP-C4-Halo-DOCK11 cells with or without HBV infection. Whole stain-free gel image is shown (left). Two representative lysates from each condition. Control; lysates from HepG2-NTCP-C4, Halo-DOCK11; lysates from HepG2-NTCP-C4-Halo-DOCK11 cells. (-); non-HBV-infected, +HBV; HBV-infected. Immunoblotting images using anti-DOCK11,  $\beta$ -catenin or  $\beta$ -Actin antibodies are shown (right). (F) Ortho view of Z-stack images of HepG2.2.15 cells co-stained with DOCK11 and  $\beta$ -Catenin antibodies. Scale bar; 10  $\mu$ m. The pseudocolor green; DOCK11, red;  $\beta$ -Catenin and blue; DAPI. White arrows; representative co-localized reactions with DOCK11 and  $\beta$ -catenin proteins.

#### 2.4. Wnt/b-catenin agonist SKL2001 strongly suppressed cccDNA and HBV-DNA levels

We subsequently examined the effect of another Wnt/b-catenin agonist, SKL2001 (5-[furan-2-yl]-N-[3-(1H-imidazol-1-yl)propyl]-1,2-oxazole-3-carboxamide) in HBV-infected cells. SKL2001 was originally discovered as a potent activator of the Wnt/b-catenin signaling pathway that disrupts axin/ $\beta$ -catenin interactions in the  $\beta$ -catenin destruction complex without affecting GSK3 $\alpha$ / $\beta$  kinase activity [33]. Treatment of cells with SKL2001 induces  $\beta$ -catenin accumulation in the cytoplasm [33,34] and it has both proliferative and inhibitory effects on cell growth [35,36]. Here, the addition of SKL2001 as a Wnt/b-catenin agonist in HBV-infected PXB and HepG2.2.15 cells resulted in a significant dose-dependent suppression of cccDNA and HBV-DNA levels, contrary to expectations (Figure 5A, 5B). For PXB cells, 10  $\mu$ M of SKL2001 showed no cytotoxicity compared to DMSO adjusted to the same concentration (0.05% in total medium); however, 100  $\mu$ M and 300  $\mu$ M of SKL2001 treatment induced significant cytotoxicity in HepG2.2.15 cells (Supplementary Figure S3). Although DMSO is believed to have relatively low toxicity, the inhibition of cell proliferation induced over 100  $\mu$ M SKL2001 treatment was due to high concentration of DMSO. Comparison analysis indicated that 10 nM entecavir treatment suppressed cccDNA the most, and 10  $\mu$ M SKL2001 administration tended to be significantly higher ( $p = 0.015$ ) compared to entecavir (Figure 5C). Conversely, no significant difference was observed in the HBV-DNA levels among the culture conditions. To investigate the effect of co-treatment with entecavir, each drug was administered to PXB cells from 1 d before HBV infection (d 0) to d 12 (Figure 6; red). The cccDNA and HBV-DNA expression levels were significantly lower in the combination treatment groups of XAV939 or SKL2001 with entecavir compared to those in the entecavir alone treatment group. Next, we examined whether the combined effect with entecavir was also observed when each drug was added 7 d after HBV infection. The combination with XAV939 was not significantly different from entecavir alone; however, the combination with SKL2001 was significantly different (Figure 6; blue). The elimination of cccDNA at the same concentration as entecavir was more efficient when it was added during the early phase of HBV infection. The combined effect of entecavir and SKL2001 treatment in reducing cccDNA and HBV-DNA levels was also observed in HepG2.2.15 cells (Supplementary Figure S4).

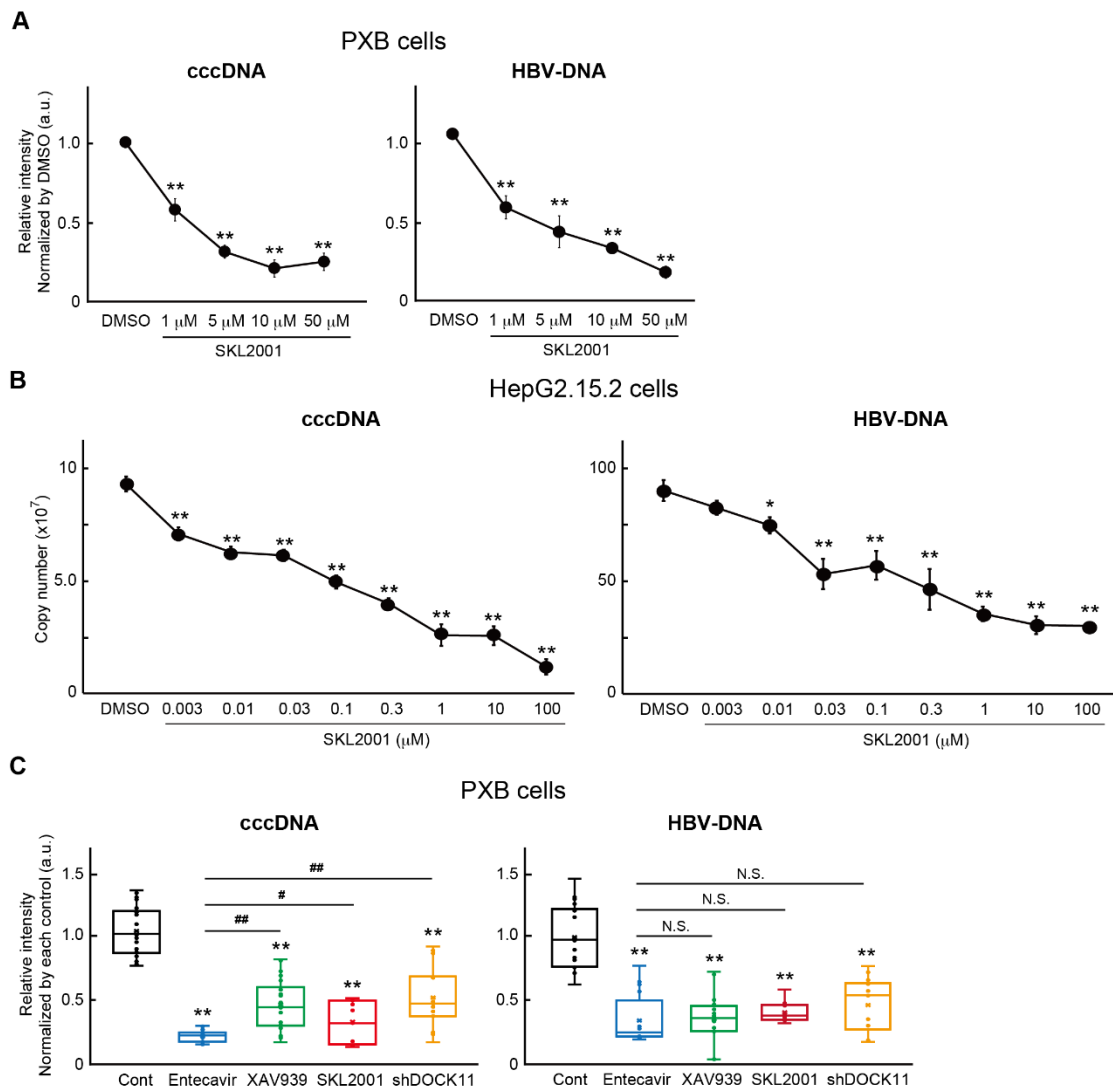


**Figure 5.** Effects of SKL2001 for eliminating of cccDNA and HBV-DNA. **(A)** The effect of Wnt/ $\beta$ -catenin agonist SKL2001 to the cccDNA and HBV-DNA expression were measured in PXB cells using qPCR. The relative intensity (arbitrary units; a.u.) was calculated by the normalization of each copy number to the 0.015% DMSO treatment groups. Bars indicate the mean  $\pm$  standard error (S.E.). \*\*,  $p < 0.01$  vs DMSO group. Number of cell culture batches (N) = 3, number of culture wells (n) = 7–18. **(B)** Dose-dependent effects of SKL2001 treatment on cccDNA and HBV-DNA copy numbers in HepG2.2.15 cells. The graph shows the mean  $\pm$  S.E. of raw copy numbers of cccDNA and HBV-DNA compared to 0.05% DMSO groups. \*,  $p < 0.05$  or \*\*,  $p < 0.01$  vs DMSO. N=3, n=5–8. **(C)** The graph shows the mean  $\pm$  S.E. of relative intensity normalized by each control condition; for instance, same volume of purified water vs 10 nM entecavir, 0.05% DMSO vs 10  $\mu$ M SKL2001 or shRNA for MOCK vs DOCK11. \*\*,  $p < 0.01$  vs each control. Cont: mean  $\pm$  S.E. of 0.05% DMSO treatment. N=3–4, n=8–21.

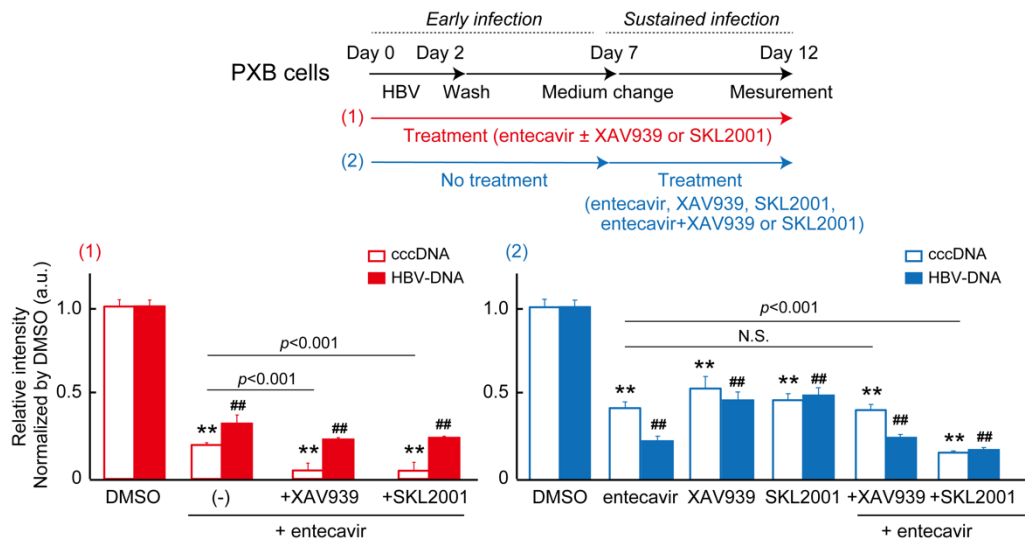


**Figure 6.** Effects of co-administration with entecavir on cccDNA and HBV-DNA levels. The upper panel shows the loading status of various inhibitors in PXB cell culture. Red (1): Co-treatment with entecavir and XAV939 or SKL2001 throughout HBV infection. Blue (2): There was no drug treatment during the first 7 d, except for HBV infection, and each inhibitor was applied for up to 5 d. The bottom bar graphs show the effects of combination treatment under different culture conditions. Y axis indicates relative intensity normalized to the copy number in the 0.05% DMSO group. Left (1): The red-bordered graph shows cccDNA and the red-filled graph shows HBV-DNA. (-): entecavir treatment alone. \*\* or ##,  $p < 0.01$  vs DMSO. The comparison among (-) vs +XAV939 or (-) vs +SKL2001 were significantly ( $p < 0.001$ ) different. N=3, n=8-10. Right (2): The blue-bordered graph shows cccDNA, and the blue graph shows HBV-DNA. \*\* or ##,  $p < 0.01$  vs DMSO. The comparison between entecavir and entecavir+XAV939 for cccDNA and HBV-DNA was not significant (N.S.). A statistically significant ( $p < 0.01$ ) relative intensity of cccDNA or HBV-DNA expression was observed in the entecavir with SKL2001 group compared to the entecavir alone treatment group. N=3, n=8.

2.5. DEGs of co-treatment effect of Wnt/b-catenin agonist SKL2001 and entecavir

RNA-seq was performed on HBV-infected PXB cells to investigate the gene expression kinetics of the combined effects of SKL2001 and entecavir (Figure. 7). Some studies showed that Notch is abundant in patients with HBV [37–39], HBx protein activates Notch signaling in HBV-HCC [40], and Notch signaling activity facilitates cccDNA transcription in HepG2.2.15.7 cells [41]. Our gene ontology analysis by using RNA-seq data indicated that 10  $\mu$ M SKL2001 administration downregulated Notch signaling (R-HAS-1912422: Pre-NOTCH Expression and Processing) compared to that in the DMSO treatment group (Figure. 7C). Co-treatment with SKL2001 and entecavir further suppressed Notch signaling (GO:0008593 regulation of the Notch signaling pathway) (Figure 6F), indicating that the combination of SKL2001 and entecavir may be effective in eliminating HBV. SKL2001 plus entecavir treatment enhanced protein phosphorylation (GO: 0006468), negative regulation of apoptosis (WP254, GO: 1900118, GO: 2001234), cell differentiation (GO: 0045596, negative regulation of cell differentiation), and endocytosis (GO: 0006897). The detailed involvement of each signaling pathway in cccDNA or HBV-DNA elimination is unknown; however, combination treatment did not activate any signals associated with cytotoxicity. RNA-seq results for non-HBV HepG2 and HepG2.2.15 cells treated with SKL2001 are shown in Supplementary Figure S5. SKL2001 treatment tended to enhance Wnt/ $\beta$ -catenin signaling; however, the effects were not significant compared to those under control culture in both cell lines. The signaling pathways accelerated by SKL2001 treatment in HepG2 and HepG2.2.15 cells were similar, indicating that the gene expression changes in HepG2.2.15 cells after the removal of HBV by SKL2001 treatment were not extremely high. Rather, SKL2001 treatment resulting in upregulated Wnt/ $\beta$ -catenin signaling contributed significantly to the changes of gene expression. The signaling pathways upregulated by

SKL2001 treatment in HBV-infected PXB cells shown in Figure. 7C differed to those in HepG2.2.15 cells, indicating a different mechanism of action for SKL2001 in HBV-infected non-cancer and cancer cells.

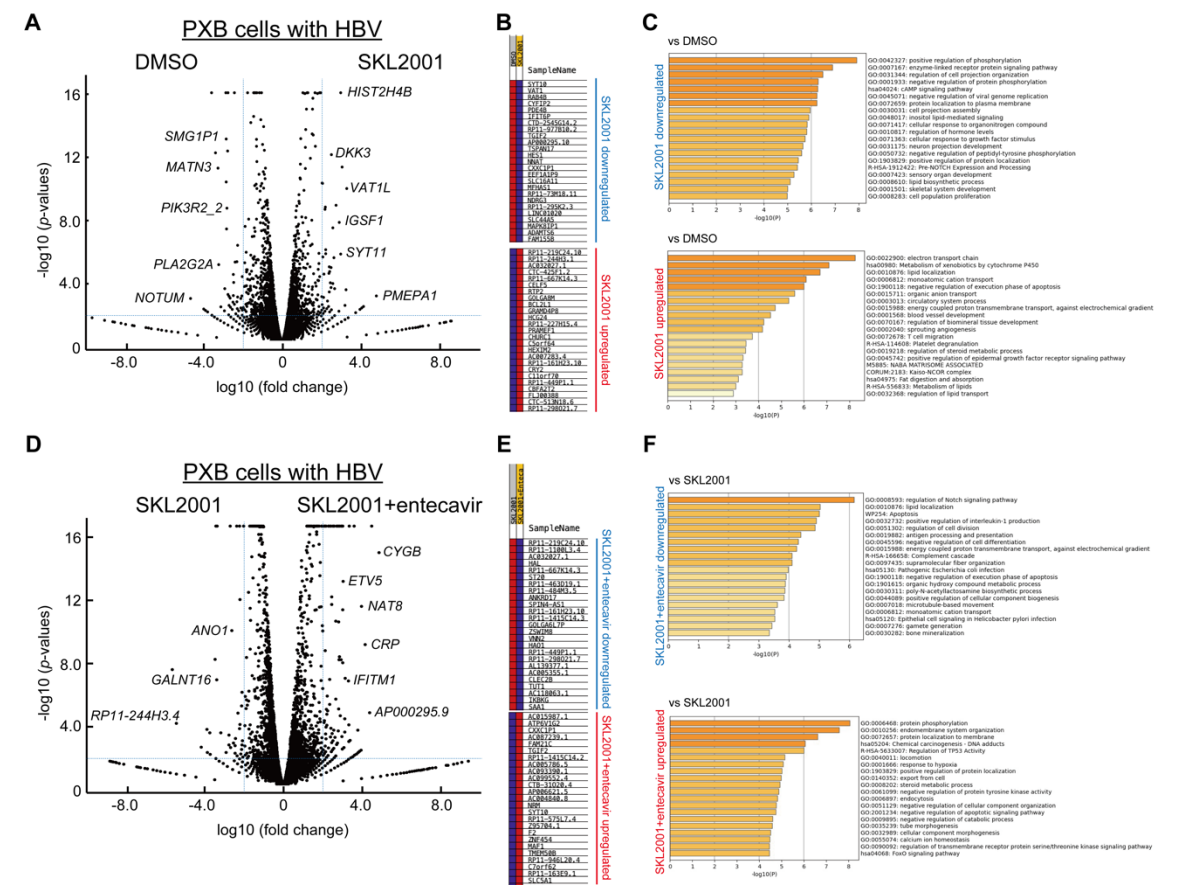


**Figure 7.** RNA-seq analysis in three different culture conditions. (A) RNA-seq data was analyzed by CLC Genomics Workbench and the DEGs between DMSO and 10  $\mu$ M SKL2001 treatment groups were visualized using a volcano map. The definition of DEGs (blue dotted lines) was  $\log_2$  FC > 1.0 and  $-\log_{10}(\text{p-value}) > 2.0$ . We used two different RNA-seq datasets obtained from different PXB cells to detect DEGs. (B) Heatmap plots of the top 50 upregulated or downregulated DEGs obtained using gene set enrichment analysis. Each heatmap shows only the top 20 extracted genes. The colors are row-normalized rank-ordered gene scores such that the maximum value for each gene is plotted in red and the minimum value is plotted in blue. “SKL2001 downregulated” is equivalent to “DMSO upregulated,” indicating these genes might be related to the maintenance of HBV in PXB cells. (C) Gene Ontology (GO) analysis using Metascape showed significantly downregulated gene functions (upper graph) and upregulated gene functions (lower graph) following SKL2001 treatment. Bars indicate  $-\log_{10}(\text{p-value})$ . (D) Volcano map between 10  $\mu$ M SKL2001 and 10  $\mu$ M SKL2001 with 10 nM entecavir treatment groups. (E) Heatmap plots of the top 20 upregulated or downregulated DEGs obtained using GSEA enrichment analysis. “SKL2001+Entecavir downregulated” means “SKL2001 treatment alone upregulated.” (F) The effect of co-treatment with SKL2001 and entecavir on signaling pathways analyzed using Metascape. Bars indicate  $-\log_{10}(\text{p-value})$ .



### 3. Discussion

The inhibition of TNKS and Wnt/ $\beta$ -catenin signaling reduced cccDNA and HBV-DNA levels in PXB and HepG2.2.15 cells. The tested Wnt/ $\beta$ -catenin agonists, except SKL2001, enhanced HBV activity. Contrary to our expectations, SKL2001 was sufficient to drastically reduce HBV infection without causing cell damage. In addition, DOCK11, which regulates the rcDNA transport from cytoplasm to nucleus [3], was co-expressed with  $\beta$ -catenin in HBV-infected cells, suggesting that the DOCK11/ $\beta$ -catenin complex with rcDNA freely translocates between nucleus and cytoplasm through the NPCs.

The association of  $\beta$ -catenin with the HBV lifecycle in normal hepatocytes may be different from that in cancer cells. HepG2 cells express a stabilized mutant  $\beta$ -catenin and the excessive activation of Wnt/ $\beta$ -catenin signaling is reported [42,43]. Wnt/ $\beta$ -catenin signaling is activated in normal hepatocytes, though aberrantly activated in HCC [44–47]. Approximately 8–30% of somatic mutations of  $\beta$ -catenin protein in HCC prevent its degradation, leading to the accumulation of mutated  $\beta$ -catenin in cytosol and transfer to the nucleus to upregulate Wnt target genes [45,47].  $\beta$ -catenin mutations are also detected in HBV-HCC [44,48] and poor survival is observed in patients with HCC with mutated  $\beta$ -catenin [44]. Cellular micro RNAs (miRNAs) regulate the expression and replication of HBV genes [46] and mutated HBx modulates Wnt/ $\beta$ -catenin signaling by affecting regulatory non-coding RNAs (ncRNAs) including miRNAs and long ncRNAs [49,50]. However, HBx deletion does not affect the ability of HBV to increase of  $\beta$ -catenin signaling in HepG2 cells [43]. Overexpression of wildtype  $\beta$ -catenin in the human hepatoma cell line Huh7 slightly increased HBV-DNA levels; however, the effects on cccDNA levels were not evaluated [13]. In general, cccDNA levels tend to decrease in HBV-HCC tissues in which mutated  $\beta$ -catenin enhanced. However, the effects of wild-type  $\beta$ -catenin or mutant  $\beta$ -catenin on cccDNA levels in cancer cells and other tumor tissue cells is unclear. Thus, the detailed mechanism underlying  $\beta$ -catenin-mediated regulation of the HBV lifecycle remains unknown. In this study, the effect of Wnt/ $\beta$ -catenin signaling inhibitors on cccDNA levels in HBV-infected PXB cells and the HBV-expressing cancer cell line HepG2.2.15 cells was identical in in vitro studies. Most reports indicate that mutant  $\beta$ -catenin levels are increased in cancer cells; however, cccDNA levels tend to be similar to or lower than those in non-tumor cells [51–54]. The larger the tumor diameter, the lower the cccDNA expression [51]. Low cccDNA levels in tumors may allow HBV to escape immune attacks. In contrast, the level of HBV-DNA expression in tumors relative to non-tumor tissues from the same liver tissue has not been established. Patient-dependent diversity occurs in HBV-DNA and cccDNA expression in tumor and non-tumor areas; however, the total copies/cell of HBV-DNA tends to increase in tumor areas [53,54]. The decrease in the amount of HBV-DNA observed in tumors is primarily associated with a decrease in non-replication of the viral genome [52]. The cccDNA/total HBV-DNA level is often discussed as the viral replication rate, and a lower percentage of viral replication is associated with liver fibrosis and poor survival in HCC [51,54]; the median cccDNA/HBV-DNA ratio in tumor or non-neoplastic liver tissue is 0.008 or 0.1, respectively. Here, the median viral replicative activity in HepG2.2.15 cells established from liver cancers was 0.1, which was similar to that in non-neoplastic liver tissue (Supplementary Figure S6). The effects of TNKS and various Wnt/ $\beta$ -catenin inhibitors on mutated  $\beta$ -catenin in cancer cells are unknown. Further studies are warranted; however, we believe the synergistic effect of inhibiting the accumulation of mutated  $\beta$ -catenin using TNKS inhibitors and reducing cccDNA and HBV-DNA expression using entecavir may inhibit HBV-derived HCC migration.

The Wnt/ $\beta$ -catenin agonist SKL2001, or 5-(Furan-2-yl)-N-(3-(1H-imidazol-1-yl)propyl)-1,2-oxazole-3-carboxamide, was first identified from a screening of 270,000 compounds as a small compound that disrupts the  $\beta$ -catenin destruction complex [33]. This inhibition of  $\beta$ -catenin phosphorylation at Ser33/37/Thr41/Ser45 may be involved in the SKL2001-mediated  $\beta$ -catenin stabilization without affecting the phosphorylation of GSK-3 $\beta$  at Ser9. Thus, SKL2001 would exert more specific Wnt modulating activity without affecting multiple other GSK3 $\beta$ -mediated signaling pathways. Activation of Wnt/ $\beta$ -catenin pathway acts as an important contributor to epithelial mesenchymal transition (EMT) and tumor progression in many cancers. The blockage of Wnt/ $\beta$ -

catenin signaling by 10 mM XAV939 treatment significantly suppressed the cell growth of HCC cell lines Huh-7, and tumor progression is enhanced by 40  $\mu$ M SKL2001-treated SMMC-7721 cells [34]. SKL2001 treatment (20  $\mu$ M) increases the protein levels of  $\beta$ -catenin in esophageal carcinoma cells, leading EMT promotion [55]. However, conflicting reports exist on the pharmacological effects of SKL2001 and its role in Wnt/ $\beta$ -catenin signaling in tumors. SKL2001 is used as a rescue for suppressed cell proliferation by decreasing  $\beta$ -catenin expression in human breast cancer cells and Huh7 cells [56,57]. SKL2001 treatment induces cytoprotective effects by suppressing cell death and releasing inflammation-related cytokines in a pancreatic ductal adenocarcinoma cell line [58]. In colon cancer spheroid cultures, 40  $\mu$ M SKL2001 suppresses tumor growth by inhibiting the G0/G1 cell cycle and affecting the association of the E-cadherin/ $\beta$ -catenin complex and cell-cell contact [35]. In our study, RNA-seq results indicated that treatment with 10  $\mu$ M SKL2001 for 10 d upregulated the Wnt/ $\beta$ -catenin signaling, and treatment with less than 10  $\mu$ M SKL2001 increased the cccDNA/HBV-DNA ratio (Supplementary Figure S6), suggesting that SKL2001 treatment might inhibit HBV-derived HCC by promoting Wnt/ $\beta$ -catenin signaling. In addition, Metascape analysis revealed that the combined effects of SKL2001 and entecavir reduced Notch signaling and suppressed cell death signaling more than treatment with SKL2001 alone in PXB cells. Notch is abundantly expressed in patients with HBV [39], and HBx activates Notch signaling in HBV-derived HCC [38]. The expression patterns of Notch signaling was reduced in the presence of entecavir in HepG2.2.15.7 cells [37]. SKL2001 may act as an inhibitor of Wnt/ $\beta$ -catenin signaling similar to XAV939 in HBV-infected cells; however, the changes in gene expression compared to those in normal hepatocytes need to be investigated. In particular, the side effects which may occur after treatment with XAV939 remain unclear because cancer-related CYP1A (cytochrome p450) family genes were upregulated in treated PXB cells compared to those in the DMSO control group (Figure 2C). Further validation of the side effects of XAV939 and SKL2001 in normal, HBV-infected, or cancer-derived hepatocytes is required.

## 4. Methods

### 4.1. Cell culture

The human liver cancer HepG2.2.15 cell line was authenticated by DNA fingerprinting in 2016. The cells were cultured onto the Collagen I coated culture well (AGC TECHNO GLASS Co. Ltd, Shizuoka, Japan) and maintained in Dulbecco modified Eagle medium/F-12, GlutaMax supplement (Thermo Fisher Scientific, Waltham, MA, USA) with 10% fetal bovine serum (BSA; Hyclone Laboratories LLC, Logan, UT, USA), 100 U/mL penicillin and 100  $\mu$ g/mL streptomycin (Thermo Fisher) and 400  $\mu$ g/mL G418, (Geneticin; Thermo Fisher). Primary human hepatocytes (PXB cells), HBV, and culture medium were purchased from PhoenixBio Co. Ltd. (Hiroshima, Japan). The transported cell lines were incubated for 6 h and then infected with HBV at 5 GEq/cell in the presence of 5% polyethylene glycol 8000 (Hampton Research, Aliso Viejo, CA, USA) for 1 – 2 d at 37°C in a humidified incubator in an atmosphere of 5% CO<sub>2</sub>. After removing the supernatant, the cells were maintained in culture medium with or without inhibitors or agonists. Four – five days after the first medium change, the supernatant was replaced with fresh culture medium, with or without each drug. Cells were used for subsequent experiments, 10 – 12 d after HBV infection, .

### 4.2. Quantification of cccDNA and HVB-DNA

Total DNA was extracted from the cells using SMITEST EX-R&D (Medical & Biological Laboratories Co. Ltd., Tokyo, Japan) according to the manufacturer's protocol. The concentration of the extracted DNA was measured using a NanoDrop spectrophotometer (Thermo Fisher). The cccDNA was generated from 1200 ng of DNA using Plasmid-Safe ATP-dependent DNase (Lucigen, Middleton, MD, USA)[59]. The 15  $\mu$ L of 1200 ng DNA, 2  $\mu$ L of 10 $\times$ Plasmid-safe buffer, 2  $\mu$ L of 25 mM ATP solution, 30 U (3  $\mu$ L) of Plasmid-Safe ATP-dependent DNase were incubated at 37°C for 45 min, following 70°C for 30 min. After cooling at 4°C , 8  $\mu$ L of cccDNA solution or same amount of DNA, 10  $\mu$ L of TaqMan Fast Universal PCR Master Mix (Applied Biosystems, Waltham, MS, USA), 0.5  $\mu$ L

of 25  $\mu$ M HBV forward primer (5'-ACTCACCAACCTCCTGTCCT-3'), 0.5  $\mu$ L of 25  $\mu$ M HBV reverse primer (5'-GACAAACGGGCAACATACCT-3') and 1  $\mu$ L of 25  $\mu$ M FAM/ZEN/IBFQ (5'-/56-FAM/TATCGCTGG/ZEN/ATGTGTCTGCGGCGT/3IABkFQ/-3', purchased from Integrated DNA Technologies Inc, Coralville, IA, USA) were mixed well. After 120 sec at 50°C and 140 sec at 95°C, 50 cycles (95°C for 3 sec and 60°C for 30 sec) of polymerase chain reaction (PCR) amplification were performed for HBV detection. From the standard HBV curve, we calculated the raw HBV copy number and normalized it for each culture condition.

#### 4.3. Western blotting

Total protein was extracted from cells and boiled at 95°C for 5 min in a loading buffer of Laemmli sample buffer with  $\beta$ -mercaptoethanol (Bio-Rad Laboratories Inc, Hercules, CA, USA). Cell lysates of HepG2-NTCP-C4 and Dox-inducible HepG2-NTCP-C4-Halo-DOCK11 cells with or without HBV infection were obtained from Prof. M. H. at Kanazawa University [4]. Each sample was loaded onto Mini-PROTEAN TGX stain-free gel (4-20% or 7.5%, Bio-Rad) with running buffer (Tris/glycine/SDS buffer, Bio-Rad). Electrophoresis was performed at 200 V for 30 min and the stain-free gel was photographed using a protein gel imaging system (ChemiDoc-Touch Imaging system, Bio-Rad) for detection of total proteins. The gel was transferred using Trans-Blot Turbo Transfer Pack (Bio-Rad) at 2.5 A for 7 min and the transferred membrane was cut into the targeted molecule sizes. After blocking with EveryBlot Blocking buffer (Bio-Rad) for 15 min, the membrane was incubated with the primary antibody overnight at 4°C, followed by three washes with Tris-Buffered Saline and 0.05% Tween-20 (TTBS) buffer. The primary antibodies were anti-TNKS (ab227471, 1:500, Abcam plc, Cambridge, UK), anti-hepatitis B virus core antigen (3HB17, 1:100, HyTest Ltd, Turku, Finland), anti-GAPDH (ab9483, 1:1000, Abcam), anti-DOCK11 (autologous, 100  $\mu$ g, obtained from Prof. K.M. in Tokyo University of Science), anti-DOCK11 (GTX55982, 1:1000, GeneTex Inc, Irvine, CA, USA), anti- $\beta$ -catenin (#9582, 1:1000, Cell Signaling Technology Inc, Danvers, MA, USA), anti- $\beta$ -catenin (ab16051, 1:1,000, Abcam) and anti- $\beta$ -actin (ab8226, 1:1000, Abcam). After three washes, the secondary goat anti-rabbit or anti-mouse IgG antibodies (170-6515 or 170-6516, 1:2000, Bio-Rad) were applied at room temperature (RT) for 1 h. After washing with TTBS, an appropriate amount of Clarity Western ECL Substrate (Bio-Rad) was added to the membrane, and the membrane was placed on a ChemiDoc Touch Imaging system (Bio-Rad) to capture chemiluminescence in auto-exposure mode.

#### 4.4. Cell proliferation assay

The Cell Proliferation Kit I (MTT based, Roche, Basel, Switzerland) was used for measurement of cell proliferation with following the manuals. In brief, 10 or 20  $\mu$ L of the MTT labeling reagent was added to each well after cells were cultured in 48 or 24-well cell plate. The culture plate was incubated for 4–5 h at 37°C, and then 100  $\mu$ L of the solubilization buffer was added. The absorbance of purple formazan crystals in each well was measured using a GloMax Discover Microplate Reader (Promega, Madison, Wisconsin, USA). The survival rate (arbitrary unit, a.u.) in each culture condition was calculated by normalization to the intensity obtained by the wavelength > 650 nm in the DMSO-treated culture (control).

#### 4.5. RNA sequencing (RNA-seq)

Total RNA in cultured cells was obtained using the RNeasy Mini Kit (Qiagen, Hilden, Germany) according to the manufacturer's instructions. RNA quality was evaluated using an Agilent 4200 TapeStation (Agilent Technologies, Santa Clara, CA, USA), and RNA concentration was measured using a Qubit 2.0 Fluorometer (Thermo Fisher). A total of 1000–4000 ng of RNA from each sample was used, and libraries for sequencing were constructed using the TruSeq Stranded mRNA Kit (Illumina, Inc., San Diego, CA, USA) according to the manufacturer's protocol. The concentration of the libraries was estimated using a KAPA Library Quantification Kit (Roche). The average library size was 350 bp. High-throughput sequencing of the samples was performed using the NextSeq

500/550 High Output Kit v2.5 (Illumina, 75 cycles pair-end, 40/40 cycles). The average number of sequence reads per sample was 23,333,374 in PXB cells and 20,649,133 in HepG2.2.15 cells. Bulk RNA-Seq results were analyzed using the CLC Genomics Workbench Version 12.0.2 (Filigen Inc., Nagoya, Japan). The raw transcript per million (TPM) data obtained from RNA-seq are provided in Supplementary Data. Target gene sets were analyzed using gene set enrichment analysis (GSEA) [60] and the gene ontology enrichment analysis tool Metascape [23].

#### 4.6. Short-hairpin RNA (shRNA)

The MISSION LentiPlex Human shRNA pooled library (Sigma-Aldrich Co., St. Louis, MO, USA) was used to generate lentiviruses with shRNA plasmids targeting CTNNB1 and NUP50 in PXB cells. The validated clone ID of each particle were TCRN0000290262 ( $0.74 \times 10^7$  TU/mL) and TRCN0000160160 ( $1.5 \times 10^7$  TU/mL). As a negative or positive control, MISSION TRC2 Control Transduction Particle puro Non-Mammalian shRNA#1 (SHC202V,  $4.6 \times 10^7$  TU/mL) or MISSION TRC2 Control Transduction Particle puro-CMV-TurboGFP (SHC203V,  $1.6 \times 10^8$  TU/mL) was used. PXB cells were infected with hexadimethrine bromide ( $8 \mu\text{g/mL}$ ) and four multiplicity of infection (MOI) of each particle for 1 d. Virus-containing media were aspirated and fresh complete media were added, and the cultures were incubated for 10 d with medium change at d 5. Total RNA was extracted using the RNeasy Mini Kit and purified RNA samples were processed into single-stranded complementary DNA (cDNA) using oligo (dT) and random primers (Takara Bio, Shiga, Japan) and SuperScript III Reverse Transcriptase (Invitrogen, Grand Island, NY, USA). The DNA concentration was measured using a NanoDrop and Qubit 2.0 Fluorometer. Synthesized cDNA was amplified by real-time PCR system QuantStudio3 (Thermo Fisher) using SYBR Green (Takara Bio) with specific primers; human CTNNB1-forward (3'-ATGGACGTGGGCGAACTTC-5') and human CTNNB1-reverse (5'-TTTGTTCGACGCATCTTCT-3') or human NUP50-forward (5'-TCTGGAGGAGGACGCTTTTCT-3') and human NUP50-reverse (5'-GGGGCACTGGTTATGTTGTTT-3') or human GAPDH-forward (5'-GCGCCCAATACGACCAA-3') or human GAPDH-reverse (5'-CTCTCTGCTCCTCCTGTTC-3') to confirm the validated shRNA knockdown efficiency.

#### 4.7. Immunoprecipitation (IP) Assay

The IP assays of DOCK11 or  $\beta$ -catenin were performed using the Universal Magnetic CO-IP kit (Active Motif Inc, Carlsbad, CA, USA), following the manufacturer's instruction. Briefly, cultured cells were harvested as cell pellets, and whole-cell extraction was performed. Cell lysates were incubated with  $10 \mu\text{g}$  of anti-rabbit DOCK11 antibody (A301-638A, Bethyl Laboratories Inc, Montgomery, TX, USA) or  $10 \mu\text{g}$  of anti- $\beta$ -catenin (#9582, Cell Signaling Technology) or rabbit IgG overnight at  $4^\circ\text{C}$  on a rotator. After centrifuging, the liquid was collected and Protein G magnetic beads were added, and then it was incubated for 3 h at  $4^\circ\text{C}$  on a rotator. After subsequent washing four times with complete/CO-IP buffer (Active Motif), bead pellets were resuspended in the loading buffer containing  $\beta$ -mercaptoethanol (Bio-Rad) and boiled at  $95^\circ\text{C}$  for 5 min before western blotting. The cell lysate obtained by IP with rabbit IgG was used as the control (input).

#### 4.8. Immunofluorescence microscopy and fluorescence imaging

HepG2.2.15 cells were cultured onto the Collagen I coated cover glasses (AGC TECHNO GLASS Co.) in culture-wells, and cover glasses were rinsed once using PBS with 10% BSA (washing buffer) and fixed for 30 min with 4% polyformaldehyde (PFA; FUJIFILM Wako Pure Chemical Co., Osaka, Japan). The cover glasses were then permeabilized using 1% Triton 100-X (Sigma-Aldrich) in PBS at RT for 10 min. The cover glasses were blocked with a blocking buffer Blocking One-P (NACALAI TESQUE Inc, Kyoto, Japan) for 30 min at  $37^\circ\text{C}$ . The primary antibodies anti-rabbit polyclonal DOCK11 (1:200, autologous or 1:200, GeneTex), were applied overnight at  $4^\circ\text{C}$ . The secondary antibodies, anti-rabbit Alexa Fluor 488 (1:2000, Thermo Fisher) were incubated for 30 min at  $37^\circ\text{C}$ . Then, the same



procedures were applied to the DOCK11-stained cover glasses using primary antibodies anti-mouse monoclonal  $\beta$ -Catenin (ab237983, 1:100, Abcam) and the secondary antibody anti-mouse Alexa Fluor 594 (1:2000, Thermo Fisher) under shading conditions. The SlowFade Diamond Antifade Mountant with DAPI (Thermo Fisher) and an encapsulating agent were added to the cover glasses, and images were acquired using ZEISS LSM900 Airyscan 2 (Carl Zeiss, Oberkochen, Germany). The acquisition conditions were 63 $\times$  oil lens, excitation channels; 405, 488, 561, emission channels; DAPI, Alexa Fluor 488 and Alexa Fluor 594, pinhole to 1 Airy Unit, master gain; 600 – 800, digital offset; 0, digital gain; 3.0 – 7.0, averaging 4 $\times$ , scan speed; Max, z-stack mode; interval 1  $\mu$ m and 17 slices.

#### 4.9. Statistical Analyses

Data were collected in Microsoft Excel and statistically analyzed using the data analysis tool. Data is expressed as the mean and standard error (mean  $\pm$  S.E.). For each culture condition, significant differences were evaluated using one-way analysis of variance (ANOVA) followed by an unpaired t-test. Statistical significance was set at  $p < 0.05$ .

## 5. Conclusion

Treatment with XAV939 or SKL2001 inhibited of Wnt/ $\beta$ -catenin signaling via reducing cccDNA and HBV-DNA levels in HBV-infected PXB and HepG2.2.15 cells. The combined effects of these agents with entecavir are promising. Thus, XAV939 and SKL2001 may be novel drug candidates for eliminating HBV by suppressing HBV-derived HCC progression.

**Supplementary Materials:** The following supporting information can be downloaded at the website of this paper posted on Preprints.org.

**Author Contributions:** **Atsushi Ishida, Sadahiro Iwabuchi;** Conceptualization (equal); formal analysis (lead); methodology (equal); validation (equal); writing—original draft (lead). **Kazuhisa Murai, Takayoshi Shirasaki;** Methodology (equal); resources (supporting); validation (supporting). **Kazuyuki Kuroki;** Methodology (supporting); resources (equal). **Yiang-Yi Li;** Conceptualization (supporting); methodology (supporting); resources (supporting). **Tetsuro Shimakami;** Resource (Supporting information). **Koki Nio and Kazunori Kawaguchi;** Resource (Supporting information). **Tadashi Imafuku;** Formal analysis (supporting information). **Satoru Ito;** Resource (supporting); funding acquisition (equal). **Taro Yamashita;** Supervision (equal). **Shuichi Kaneko;** Supervision (equal), funding acquisition (equal). **Kouji Matsushima;** resources (equal); supervision (equal); funding acquisition (equal). **Masao Honda;** resources (equal); supervision (equal); funding acquisition (equal). **Shinichi Hashimoto;** Conceptualization (equal), supervision (equal), funding acquisition (equal), writing—original draft (supporting), project administration (lead).

**Funding:** This study was supported by Japan Agency for Medical Research and Development (AMED) Grants 17fk0310110h0001, 20fk0310110s8003, 21fk0310110s8005, 22fk0310514s0101, JP23fk0310514, JP23fk0210129, JP23fk0210140, and JP25fk0310539).

**Acknowledgments:** We thank Yuriko Hishida, Mayuko Hatai, Michi Isono, and Yu Kamide for technical assistance with the experiments. We would like to thank Editage (www.editage.com) for English language editing.

**Conflicts of Interest:** The authors declare that this study was conducted in the absence of any commercial or financial relationships that could be construed as potential conflicts of interest.

## References

1. Nassal, M., HBV cccDNA: viral persistence reservoir and key obstacle for a cure of chronic hepatitis B. *Gut* **2015**, 64, (12), 1972–84.

2. Zhang, Y. Y.; Zhang, B. H.; Theele, D.; Litwin, S.; Toll, E.; Summers, J., Single-cell analysis of covalently closed circular DNA copy numbers in a hepadnavirus-infected liver. *Proc Natl Acad Sci U S A* **2003**, 100, (21), 12372-7.
3. Doan, P. T. B.; Nio, K.; Shimakami, T.; Kuroki, K.; Li, Y. Y.; Sugimoto, S.; Takayama, H.; Okada, H.; Kaneko, S.; Honda, M.; Yamashita, T., Super-Resolution Microscopy Analysis of Hepatitis B Viral cccDNA and Host Factors. *Viruses* **2023**, 15, (5).
4. Li, Y. Y.; Kuroki, K.; Shimakami, T.; Murai, K.; Kawaguchi, K.; Shirasaki, T.; Nio, K.; Sugimoto, S.; Nishikawa, T.; Okada, H.; Orita, N.; Takayama, H.; Wang, Y.; Thi Bich, P. D.; Ishida, A.; Iwabuchi, S.; Hashimoto, S.; Shimaoka, T.; Tabata, N.; Watanabe-Takahashi, M.; Nishikawa, K.; Yanagawa, H.; Seiki, M.; Matsushima, K.; Yamashita, T.; Kaneko, S.; Honda, M., Hepatitis B Virus Utilizes a Retrograde Trafficking Route via the Trans-Golgi Network to Avoid Lysosomal Degradation. *Cell Mol Gastroenterol Hepatol* **2023**, 15, (3), 533-558.
5. Ide, M.; Tabata, N.; Yonemura, Y.; Shirasaki, T.; Murai, K.; Wang, Y.; Ishida, A.; Okada, H.; Honda, M.; Kaneko, S.; Doi, N.; Ito, S.; Yanagawa, H., Guanine nucleotide exchange factor DOCK11-binding peptide fused with a single chain antibody inhibits hepatitis B virus infection and replication. *J Biol Chem* **2022**, 298, (7), 102097.
6. Hashimoto, S.; Shirasaki, T.; Yamashita, T.; Iwabuchi, S.; Suzuki, Y.; Takamura, Y.; Ukita, Y.; Deshimaru, S.; Okayama, T.; Ikeo, K.; Kuroki, K.; Kawaguchi, K.; Mizukoshi, E.; Matsushima, K.; Honda, M.; Kaneko, S., DOCK11 and DENND2A play pivotal roles in the maintenance of hepatitis B virus in host cells. *PLoS One* **2021**, 16, (2), e0246313.
7. Yanagawa, H., Exploration of the origin and evolution of globular proteins by mRNA display. *Biochemistry* **2013**, 52, (22), 3841-51.
8. Gibson, B. A.; Kraus, W. L., New insights into the molecular and cellular functions of poly(ADP-ribose) and PARPs. *Nat Rev Mol Cell Biol* **2012**, 13, (7), 411-24.
9. Zhang, Y.; Liu, S.; Mickanin, C.; Feng, Y.; Charlat, O.; Michaud, G. A.; Schirle, M.; Shi, X.; Hild, M.; Bauer, A.; Myer, V. E.; Finan, P. M.; Porter, J. A.; Huang, S. M.; Cong, F., RNF146 is a poly(ADP-ribose)-directed E3 ligase that regulates axin degradation and Wnt signalling. *Nat Cell Biol* **2011**, 13, (5), 623-9.
10. Yang, E.; Tacchelly-Benites, O.; Wang, Z.; Randall, M. P.; Tian, A.; Benchabane, H.; Freemantle, S.; Pikielny, C.; Tolwinski, N. S.; Lee, E.; Ahmed, Y., Wnt pathway activation by ADP-ribosylation. *Nat Commun* **2016**, 7, 11430.
11. Kimelman, D.; Xu, W., beta-catenin destruction complex: insights and questions from a structural perspective. *Oncogene* **2006**, 25, (57), 7482-91.
12. Liu, X.; Rubin, J. S.; Kimmel, A. R., Rapid, Wnt-induced changes in GSK3beta associations that regulate beta-catenin stabilization are mediated by Galpha proteins. *Curr Biol* **2005**, 15, (22), 1989-97.
13. Tarnow, G.; McLachlan, A., Selective effect of beta-catenin on nuclear receptor-dependent hepatitis B virus transcription and replication. *Virology* **2022**, 571, 52-58.
14. Tarnow, G.; McLachlan, A., beta-Catenin Signaling Regulates the In Vivo Distribution of Hepatitis B Virus Biosynthesis across the Liver Lobule. *J Virol* **2021**, 95, (20), e0078021.
15. Zhao, R.; Wang, T. Z.; Kong, D.; Zhang, L.; Meng, H. X.; Jiang, Y.; Wu, Y. Q.; Yu, Z. X.; Jin, X. M., Hepatoma cell line HepG2.2.15 demonstrates distinct biological features compared with parental HepG2. *World J Gastroenterol* **2011**, 17, (9), 1152-9.
16. Yamasaki, C.; Tateno, C.; Aratani, A.; Ohnishi, C.; Katayama, S.; Kohashi, T.; Hino, H.; Marusawa, H.; Asahara, T.; Yoshizato, K., Growth and differentiation of colony-forming human hepatocytes in vitro. *J Hepatol* **2006**, 44, (4), 749-57.
17. Li, N.; Wang, Y.; Neri, S.; Zhen, Y.; Fong, L. W. R.; Qiao, Y.; Li, X.; Chen, Z.; Stephan, C.; Deng, W.; Ye, R.; Jiang, W.; Zhang, S.; Yu, Y.; Hung, M. C.; Chen, J.; Lin, S. H., Tankyrase disrupts metabolic homeostasis and promotes tumorigenesis by inhibiting LKB1-AMPK signalling. *Nat Commun* **2019**, 10, (1), 4363.
18. Narwal, M.; Koivunen, J.; Haikarainen, T.; Obaji, E.; Legala, O. E.; Venkannagari, H.; Joensuu, P.; Pihlajaniemi, T.; Lehtio, L., Discovery of tankyrase inhibiting flavones with increased potency and isoenzyme selectivity. *J Med Chem* **2013**, 56, (20), 7880-9.

19. Norum, J. H.; Skarpen, E.; Brech, A.; Kuiper, R.; Waaler, J.; Krauss, S.; Sorlie, T., The tankyrase inhibitor G007-LK inhibits small intestine LGR5(+) stem cell proliferation without altering tissue morphology. *Biol Res* **2018**, 51, (1), 3.
20. Thorsell, A. G.; Ekblad, T.; Karlberg, T.; Low, M.; Pinto, A. F.; Tresaugues, L.; Moche, M.; Cohen, M. S.; Schuler, H., Structural Basis for Potency and Promiscuity in Poly(ADP-ribose) Polymerase (PARP) and Tankyrase Inhibitors. *J Med Chem* **2017**, 60, (4), 1262-1271.
21. Waaler, J.; Machon, O.; Tumova, L.; Dinh, H.; Korinek, V.; Wilson, S. R.; Paulsen, J. E.; Pedersen, N. M.; Eide, T. J.; Machonova, O.; Gradl, D.; Voronkov, A.; von Kries, J. P.; Krauss, S., A novel tankyrase inhibitor decreases canonical Wnt signaling in colon carcinoma cells and reduces tumor growth in conditional APC mutant mice. *Cancer Res* **2012**, 72, (11), 2822-32.
22. Al-Dhfyhan, A.; Alhoshani, A.; Korashy, H. M., Aryl hydrocarbon receptor/cytochrome P450 1A1 pathway mediates breast cancer stem cells expansion through PTEN inhibition and beta-Catenin and Akt activation. *Mol Cancer* **2017**, 16, (1), 14.
23. Zhou, Y.; Zhou, B.; Pache, L.; Chang, M.; Khodabakhshi, A. H.; Tanaseichuk, O.; Benner, C.; Chanda, S. K., Metascape provides a biologist-oriented resource for the analysis of systems-level datasets. *Nat Commun* **2019**, 10, (1), 1523.
24. Huang, S. M.; Mishina, Y. M.; Liu, S.; Cheung, A.; Stegmeier, F.; Michaud, G. A.; Charlat, O.; Wiellet, E.; Zhang, Y.; Wiessner, S.; Hild, M.; Shi, X.; Wilson, C. J.; Mickanin, C.; Myer, V.; Fazal, A.; Tomlinson, R.; Serluca, F.; Shao, W.; Cheng, H.; Shultz, M.; Rau, C.; Schirle, M.; Schlegl, J.; Ghidelli, S.; Fawell, S.; Lu, C.; Curtis, D.; Kirschner, M. W.; Lengauer, C.; Finan, P. M.; Tallarico, J. A.; Bouwmeester, T.; Porter, J. A.; Bauer, A.; Cong, F., Tankyrase inhibition stabilizes axin and antagonizes Wnt signalling. *Nature* **2009**, 461, (7264), 614-20.
25. Waaler, J.; Machon, O.; von Kries, J. P.; Wilson, S. R.; Lundenes, E.; Wedlich, D.; Gradl, D.; Paulsen, J. E.; Machonova, O.; Dembinski, J. L.; Dinh, H.; Krauss, S., Novel synthetic antagonists of canonical Wnt signaling inhibit colorectal cancer cell growth. *Cancer Res* **2011**, 71, (1), 197-205.
26. Lu, D.; Choi, M. Y.; Yu, J.; Castro, J. E.; Kipps, T. J.; Carson, D. A., Salinomycin inhibits Wnt signaling and selectively induces apoptosis in chronic lymphocytic leukemia cells. *Proc Natl Acad Sci U S A* **2011**, 108, (32), 13253-7.
27. Liu, J.; Wu, X.; Mitchell, B.; Kintner, C.; Ding, S.; Schultz, P. G., A small-molecule agonist of the Wnt signaling pathway. *Angew Chem Int Ed Engl* **2005**, 44, (13), 1987-90.
28. Wang, S.; Yin, J.; Chen, D.; Nie, F.; Song, X.; Fei, C.; Miao, H.; Jing, C.; Ma, W.; Wang, L.; Xie, S.; Li, C.; Zeng, R.; Pan, W.; Hao, X.; Li, L., Small-molecule modulation of Wnt signaling via modulating the Axin-LRP5/6 interaction. *Nat Chem Biol* **2013**, 9, (9), 579-85.
29. Fagotto, F.; Gluck, U.; Gumbiner, B. M., Nuclear localization signal-independent and importin/karyopherin-independent nuclear import of beta-catenin. *Curr Biol* **1998**, 8, (4), 181-90.
30. Matsuura, Y.; Stewart, M., Nup50/Npap60 function in nuclear protein import complex disassembly and importin recycling. *EMBO J* **2005**, 24, (21), 3681-9.
31. Chen, C.; Wang, J. C.; Pierson, E. E.; Keifer, D. Z.; Delaleau, M.; Gallucci, L.; Cazenave, C.; Kann, M.; Jarrold, M. F.; Zlotnick, A., Importin beta Can Bind Hepatitis B Virus Core Protein and Empty Core-Like Particles and Induce Structural Changes. *PLoS Pathog* **2016**, 12, (8), e1005802.
32. Soderholm, J. F.; Bird, S. L.; Kalab, P.; Sampathkumar, Y.; Hasegawa, K.; Uehara-Bingen, M.; Weis, K.; Heald, R., Importazole, a small molecule inhibitor of the transport receptor importin-beta. *ACS Chem Biol* **2011**, 6, (7), 700-8.
33. Gwak, J.; Hwang, S. G.; Park, H. S.; Choi, S. R.; Park, S. H.; Kim, H.; Ha, N. C.; Bae, S. J.; Han, J. K.; Kim, D. E.; Cho, J. W.; Oh, S., Small molecule-based disruption of the Axin/beta-catenin protein complex regulates mesenchymal stem cell differentiation. *Cell Res* **2012**, 22, (1), 237-47.
34. Liao, S.; Chen, H.; Liu, M.; Gan, L.; Li, C.; Zhang, W.; Lv, L.; Mei, Z., Aquaporin 9 inhibits growth and metastasis of hepatocellular carcinoma cells via Wnt/beta-catenin pathway. *Aging (Albany NY)* **2020**, 12, (2), 1527-1544.

35. Ohashi, W.; Yamamine, N.; Imura, J.; Hattori, Y., SKL2001 suppresses colon cancer spheroid growth through regulation of the E-cadherin/beta-Catenin complex. *Biochem Biophys Res Commun* **2017**, 493, (3), 1342-1348.
36. Zhijun, Z.; Jingkan, H., MicroRNA-520e suppresses non-small-cell lung cancer cell growth by targeting Zbtb7a-mediated Wnt signaling pathway. *Biochem Biophys Res Commun* **2017**, 486, (1), 49-56.
37. Wang, Z.; Kawaguchi, K.; Honda, M.; Sakai, Y.; Yamashita, T.; Mizukoshi, E.; Kaneko, S., Distinct notch signaling expression patterns between nucleoside and nucleotide analogues treatment for hepatitis B virus infection. *Biochem Biophys Res Commun* **2018**, 501, (3), 682-687.
38. Wang, F.; Zhou, H.; Xia, X.; Sun, Q.; Wang, Y.; Cheng, B., Activated Notch signaling is required for hepatitis B virus X protein to promote proliferation and survival of human hepatic cells. *Cancer Lett* **2010**, 298, (1), 64-73.
39. Pei, J.; Tang, Z.; Zang, G.; Yu, Y., Blockage of Notch1 signaling modulates the T-helper (Th)1/Th2 cell balance in chronic hepatitis B patients. *Hepatol Res* **2010**, 40, (8), 799-805.
40. Gao, J.; Xiong, Y.; Wang, Y.; Wang, Y.; Zheng, G.; Xu, H., Hepatitis B virus X protein activates Notch signaling by its effects on Notch1 and Notch4 in human hepatocellular carcinoma. *Int J Oncol* **2016**, 48, (1), 329-37.
41. Wang, Z.; Kawaguchi, K.; Honda, M.; Hashimoto, S.; Shirasaki, T.; Okada, H.; Orita, N.; Shimakami, T.; Yamashita, T.; Sakai, Y.; Mizukoshi, E.; Murakami, S.; Kaneko, S., Notch signaling facilitates hepatitis B virus covalently closed circular DNA transcription via cAMP response element-binding protein with E3 ubiquitin ligase-modulation. *Sci Rep* **2019**, 9, (1), 1621.
42. Cha, M. Y.; Kim, C. M.; Park, Y. M.; Ryu, W. S., Hepatitis B virus X protein is essential for the activation of Wnt/beta-catenin signaling in hepatoma cells. *Hepatology* **2004**, 39, (6), 1683-93.
43. von Olshausen, G.; Quasdorff, M.; Bester, R.; Arzberger, S.; Ko, C.; van de Klundert, M.; Zhang, K.; Odenthal, M.; Ringelhan, M.; Niessen, C. M.; Protzer, U., Hepatitis B virus promotes beta-catenin-signalling and disassembly of adherens junctions in a Src kinase dependent fashion. *Oncotarget* **2018**, 9, (74), 33947-33960.
44. Kumar, S.; Nadda, N.; Quadri, A.; Kumar, R.; Paul, S.; Tanwar, P.; Gamanagatti, S.; Dash, N. R.; Saraya, A.; Shalimar; Nayak, B., Assessments of TP53 and CTNNB1 gene hotspot mutations in circulating tumour DNA of hepatitis B virus-induced hepatocellular carcinoma. *Front Genet* **2023**, 14, 1235260.
45. He, S.; Tang, S., WNT/beta-catenin signaling in the development of liver cancers. *Biomed Pharmacother* **2020**, 132, 110851.
46. Rana, M. A.; Ijaz, B.; Daud, M.; Tariq, S.; Nadeem, T.; Husnain, T., Interplay of Wnt beta-catenin pathway and miRNAs in HBV pathogenesis leading to HCC. *Clin Res Hepatol Gastroenterol* **2019**, 43, (4), 373-386.
47. Xu, C.; Xu, Z.; Zhang, Y.; Evert, M.; Calvisi, D. F.; Chen, X., beta-Catenin signaling in hepatocellular carcinoma. *J Clin Invest* **2022**, 132, (4).
48. Chen, Z.; Tang, J.; Cai, X.; Huang, Y.; Gao, Q.; Liang, L.; Tian, L.; Yang, Y.; Zheng, Y.; Hu, Y.; Tang, N., HBx mutations promote hepatoma cell migration through the Wnt/beta-catenin signaling pathway. *Cancer Sci* **2016**, 107, (10), 1380-1389.
49. Zhang, X. D.; Wang, Y.; Ye, L. H., Hepatitis B virus X protein accelerates the development of hepatoma. *Cancer Biol Med* **2014**, 11, (3), 182-90.
50. Geng, M.; Xin, X.; Bi, L. Q.; Zhou, L. T.; Liu, X. H., Molecular mechanism of hepatitis B virus X protein function in hepatocarcinogenesis. *World J Gastroenterol* **2015**, 21, (38), 10732-8.
51. Wang, Q.; Lin, L.; Yoo, S.; Wang, W.; Blank, S.; Fiel, M. I.; Kadri, H.; Luan, W.; Warren, L.; Zhu, J.; Hiotis, S. P., Impact of non-neoplastic vs intratumoural hepatitis B viral DNA and replication on hepatocellular carcinoma recurrence. *Br J Cancer* **2016**, 115, (7), 841-7.
52. Amaddeo, G.; Cao, Q.; Ladeiro, Y.; Imbeaud, S.; Nault, J. C.; Jaoui, D.; Gaston Mathe, Y.; Laurent, C.; Laurent, A.; Bioulac-Sage, P.; Calderaro, J.; Zucman-Rossi, J., Integration of tumour and viral genomic characterizations in HBV-related hepatocellular carcinomas. *Gut* **2015**, 64, (5), 820-9.
53. Fu, S.; Li, N.; Zhou, P. C.; Huang, Y.; Zhou, R. R.; Fan, X. G., Detection of HBV DNA and antigens in HBsAg-positive patients with primary hepatocellular carcinoma. *Clin Res Hepatol Gastroenterol* **2017**, 41, (4), 415-423.



54. Wang, Q.; Fiel, M. I.; Luan, W.; Blank, S.; Kadri, H.; Kim, K. W.; Hiotis, S. P., Impact of intrahepatic hepatitis B DNA and covalently closed circular DNA on survival after hepatectomy in HBV-associated hepatocellular carcinoma patients. *Ann Surg Oncol* **2013**, 20, (12), 3761-70.
55. Xu, Q.; Li, X.; Li, Y.; Yu, J.; Yang, A., Kinesin family member 23 knockdown inhibits cell proliferation and epithelial-mesenchymal transition in esophageal carcinoma by inactivating the Wnt/beta-catenin pathway. *Funct Integr Genomics* **2023**, 23, (2), 154.
56. Liu, C.; Pan, J.; Liu, H.; Lin, R.; Chen, Y.; Zhang, C., Daphnetin inhibits the survival of hepatocellular carcinoma cells through regulating Wnt/beta-catenin signaling pathway. *Drug Dev Res* **2022**, 83, (4), 952-960.
57. An, L.; Gong, H.; Yu, X.; Zhang, W.; Liu, X.; Yang, X.; Shu, L.; Liu, J.; Yang, L., Downregulation of MAL2 inhibits breast cancer progression through regulating beta-catenin/c-Myc axis. *Cancer Cell Int* **2023**, 23, (1), 144.
58. Huang, H. L.; Tang, G. D.; Liang, Z. H.; Qin, M. B.; Wang, X. M.; Chang, R. J.; Qin, H. P., Role of Wnt/beta-catenin pathway agonist SKL2001 in Caerulein-induced acute pancreatitis. *Can J Physiol Pharmacol* **2019**, 97, (1), 15-22.
59. Gao, Y. T.; Han, T.; Li, Y.; Yang, B.; Wang, Y. J.; Wang, F. M.; Jing, X.; Du, Z., Enhanced specificity of real-time PCR for measurement of hepatitis B virus cccDNA using restriction endonuclease and plasmid-safe ATP-dependent DNase and selective primers. *J Virol Methods* **2010**, 169, (1), 181-7.
60. Mootha, V. K.; Lindgren, C. M.; Eriksson, K. F.; Subramanian, A.; Sihag, S.; Lehar, J.; Puigserver, P.; Carlsson, E.; Ridderstrale, M.; Laurila, E.; Houstis, N.; Daly, M. J.; Patterson, N.; Mesirov, J. P.; Golub, T. R.; Tamayo, P.; Spiegelman, B.; Lander, E. S.; Hirschhorn, J. N.; Altshuler, D.; Groop, L. C., PGC-1alpha-responsive genes involved in oxidative phosphorylation are coordinately downregulated in human diabetes. *Nat Genet* **2003**, 34, (3), 267-73.

**Disclaimer/Publisher's Note:** The statements, opinions and data contained in all publications are solely those of the individual author(s) and contributor(s) and not of MDPI and/or the editor(s). MDPI and/or the editor(s) disclaim responsibility for any injury to people or property resulting from any ideas, methods, instructions or products referred to in the content.